Comparison of Technetium-99m-ECD to Xenon-133 SPECT in Normal Controls and in Patients with Mild to Moderate Regional Cerebral Blood Flow Abnormalities

Michael D. Devous, Sr., J. Kelly Payne, James L. Lowe and Robert F. Leroy

Nuclear Medicine Center and Departments of Radiology and Neurology, The University of Texas Southwestern Medical Center, Dallas, Texas

Technetium-99m-1,1-ethyl cysteinate dimer (ECD) has been proposed as a "chemical microsphere" for SPECT measurement of regional cerebral blood flow (rCBF). However, its distribution has not yet been compared in humans to an established rCBF measure. Therefore, we compared the uptake and distribution of ECD with rCBF measured by ^{133}Xe SPECT in subjects with mild to moderate flow abnormalities and in normal volunteers. Blood and urine chemistries and vital signs were unchanged from pre-ECD values up to seven days postinjection. Profile plots demonstrated pattern agreement between rCBF ratios (^{133}Xe) and ECD count density ratios. A significant correlation of rCBF ratios to ECD count density ratios was observed (r = 0.77), with a slope of 0.64 and intercept of 0.36. To explore whether or not the relationship between rCBF and ECD was dependent on absolute flow, ECD region of interest data were expressed in units of ml/min/100 g by equating global CBF (^{133}Xe) and ECD global count density. A closer correlation (r = 0.88) was found for these data than for the count ratio data. The slope was closer to one (m = 0.83) and the intercept was closer to zero (b = 8.2). Also, a significant correlation was observed between ECD-derived rCBF and ^{133}Xe rCBF in the lesion area (r = 0.92) for patients with well-demarcated rCBF lesions. The slope (0.80) suggested a slight underestimation of lesion flow by ECD. Finally, ECD clearance from cortical gray matter ROIs derived from high-resolution scans from 1 to 4 hr postinjection was slow (2.4%/hr). In summary, ECD is a safe and effective marker of regional cerebral perfusion. The distribution of ECD is linearly related to rCBF measured by ^{133}Xe SPECT, although our data suggest a mild underestimation of flow at the high end of the normal range.

J Nucl Med 1993; 34:754–761

Regional cerebral blood flow (rCBF) was initially measured by Kety and Schmidt (*1*) using the inert-gas nitrous oxide method following the Fick principle (*2*). This technique was replaced by both two-dimensional and tomographic inert-gas rCBF measurements using ^{133}Xe. However, to measure rCBF by single-photon emission tomography (SPECT) with single-head rotating gamma cameras, it was necessary to develop tracers with a stable in vivo distribution. Presently there are three radiotracers approved by the Food and Drug Administration for SPECT brain blood flow imaging: ^{123}I-p-iodo-N-isopropylamphetamine (^{123}I-IMP) (*3*), ^{99m}Tc-hexamethylpropyleneamine oxime (^{99m}Tc-HMPAO) (*4,5*) and ^{133}Xe (*6*). Iodine-123-IMP and ^{99m}Tc-HMPAO cross the blood-brain barrier (BBB), distribute in proportion to brain blood flow and are trapped within the brain by metabolism of the ligand or conformational changes due to a pH differential between blood and brain. Tracers of this type are commonly referred to as "chemical microspheres." Xenon-133 also crosses the BBB but is not trapped. The dynamic transit of ^{133}Xe can be modeled to yield a quantitative rCBF measurement (ml/min/100 g). Advantages and disadvantages of these three radiopharmaceuticals have been previously described in detail (*7–14*).

A new class of radiopharmaceuticals being evaluated for brain blood flow imaging is diamine dithiol (N_2S_2) chelates (*15*). These compounds form pure, stable and neutral lipophilic complexes with ^{99m}Tc (*16*). One such agent, ^{99m}Tc-1,1-ethyl cysteinate dimer (ECD), has been evaluated in clinical trials and is under FDA review for an NDA. ECD has selective brain uptake in rhesus monkeys, cynomolgus monkeys and humans, having 95% peak uptake 20 sec after intravenous injection (*16*). ECD is rapidly metabolized in the brain to a polar product (*16,17*) and 5% of the injected dose is retained. ECD and its metabolites rapidly clear the blood, yielding high target-to-background imaging characteristics soon after injection.

In the present investigation, the uptake and distribu-

Received Oct. 6, 1992; revision accepted Jan. 18, 1993.

For correspondence or reprints contact: Dr. Michael D. Devous, Sr., Nuclear Medicine Center, UT Southwestern Medical Center, 5323 Harry Hines Blvd., Dallas, TX 75235-9061.

tion of ECD was compared with rCBF measured by ^{133}Xe SPECT in subjects with mild to moderate flow abnormalities and in normal volunteers. Validation in patients with mild to moderate rCBF abnormalities differs from validation under circumstances of severe brain blood flow abnormalities (e.g., stroke). Correlations with true rCBF obtained when contrasting uptake in normal regions to that in an infarct may be misleading since the flow differences are so large. The current study was designed to determine if ECD could accurately depict rCBF alterations over a smaller range, which might be relevant in psychiatric and neurologic disorders other than strokes. In addition, vital signs and blood and urine chemistry were assessed prior to and up to seven days after ECD injection as part of a safety evaluation. Finally, the clearance rate of ECD from the brain over time was measured in a subset of subjects.

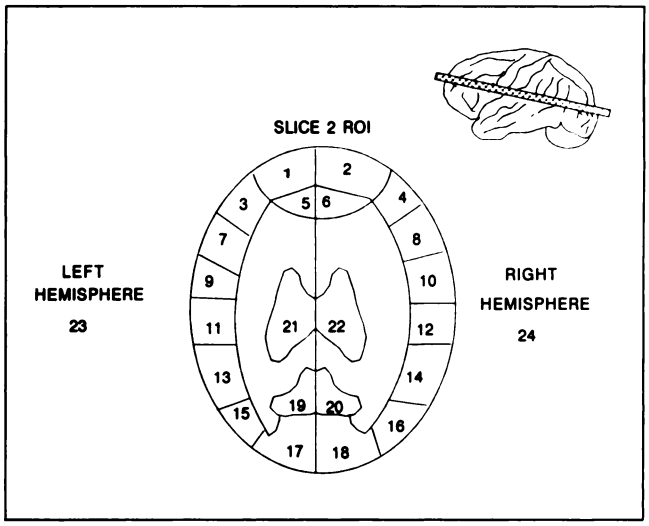

FIGURE 1. ROI within the slice 6 cm above the CML (slice 2) and relative position of the slice within brain.

MATERIALS AND METHODS

Subjects

Subjects in this study included seven neurologically and psychiatrically normal volunteers (three males, four females, age range 24–60 yr) and 11 patients with mild to moderate perfusion deficits. Patients ranged in age from 22 to 75 yr and included two males with hypertension, one female with Parkinson's disease, five males and one female with epilepsy and two females with minor chronic stroke. All subjects provided informed consent as approved by the Institutional Review Board of The University of Texas Southwestern Medical Center.

Kit Preparation

ECD (E.I. Du Pont de Nemours & Co., N. Billerica, MA) was supplied in two parts, A and B. Part A contained lyophilized ECD-2HCL (0.9 mg), stannous chloride dihydrate (0.072 mg), sodium EDTA dihydrate (0.36 mg) and mannitol (24 mg) at a pH of 2.5–2.9. Part B contained a 1.0 ml aqueous solution of Na_2HPO_4-$7H_2O$ (4.1 mg) and NaH_2PO_4-$7H_2O$ (0.46 mg) at a pH of 7.2–8.0. Vial A was reconstituted with 1.5 ml of sterile physiological saline. First, 1.0 ml of $^{99m}TcO_4^-$ (50 mCi) was added to vial B, then 1.0 ml from the reconstituted vial A was added to vial B and allowed to stand for 30 min.

Radiopharmaceutical Purity

Chromatography was performed on a 1" × 3" Whatman RP-C18 glass thin-layer chromatography plate (*16*). Lines were drawn 1.5 cm and 7.5 cm from the bottom edge. One drop of alcohol and one drop (100 μCi) from the prepared mixture in vial B were placed 1.5 cm from the bottom of the plate. The spot was dried and placed in a pre-equilibrated sealed jar containing acetone and 0.5 *M* ammonium acetate (3:2 v/v, pH 4.0) and the solvent was allowed to migrate to the 7.5-cm line. The plate was removed, dried and the amount of radioactivity at the origin and the 7.5-cm line was determined by planar gamma camera imaging. Radioactivity at each location was divided by the total activity to establish the percent activity of each region. Since the ECD complex does not migrate from the origin, the migrating fraction represents free $^{99m}TcO_4^-$. The kit was discarded if purity was <90%.

Study Protocol

Vital signs (blood pressure and heart rate) and blood and urine samples were taken 1–7 days before ECD administration and again at 1, 6, 24 and 48 hr and 7 days after SPECT imaging. Blood and urine samples were submitted to a commercial laboratory for routine evaluations and included SMAC 25, complete blood count, microscopic urinalysis, prothrombin time and partial thromboplastin time. Subjects were questioned at each sampling period about adverse reactions to ECD or the procedure.

Regional cerebral blood flow was determined by dynamic SPECT measurements of the cerebral transit of ^{133}Xe according to methods previously described (*18*) using the Tomomatic 64 (Medimatic A/S, Copenhagen, Denmark). At the time of the study, subjects were prepared by placing marks on the left side of their face (using a template for positioning purposes) and measuring head diameter (anterior to posterior and right to left) with calipers at 2, 6 and 10 cm above and parallel to the canthomeatal line (CML). Subjects were placed supine and positioned so their heads were inside a plastic shield that lined the detection space. An intravenous line was placed in the antecubital vein of each subject for the administration of ^{99m}Tc-ECD complex. Subjects were positioned so that slices were obtained 2, 6 and 10 cm above and parallel to the CML (Fig. 1). A nose clip was placed to prevent exhalation of ^{133}Xe gas through the nasal cavities and a mouth piece connected to the instrument was placed in the subject's mouth. After a 2-min adaptation period, subjects were administered 10 mCi of ^{133}Xe in air for 1 min, followed by a 3-min washout period.

At the conclusion of the ^{133}Xe study and without moving the subject, 20 mCi of ^{99m}Tc-ECD was administered intravenously followed by a saline flush. The energy window of the Tomomatic 64 was adjusted for ^{99m}Tc and, after a 15-min delay postinjection, a 4-min static acquisition was conducted using the same high-sensitivity low-resolution collimators used for ^{133}Xe. Thus, the same slices at the same resolution were imaged for both ^{133}Xe and ECD in all subjects. All comparisons between ECD and ^{133}Xe were derived from these data.

Subjects were then studied using a high-resolution SPECT tomograph (Prism 3000-S, Picker, Cleveland, OH). They were scanned in the supine position using the step and shoot tech-

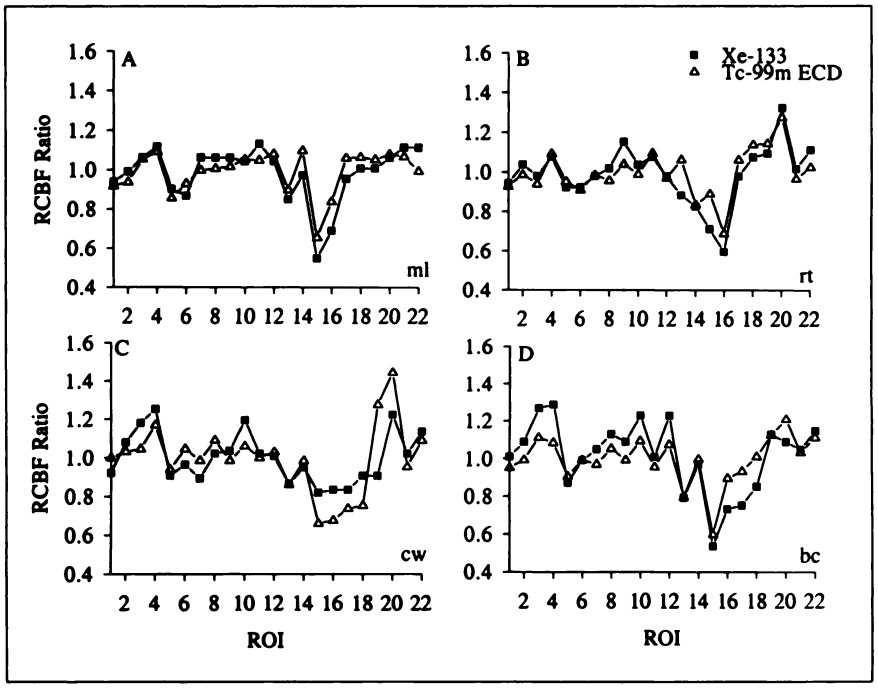

FIGURE 2. Profile plots comparing rCBF (^{133}Xe) ratios and ECD count density ratios for two subjects with "close" relationships (A and B) and for two subjects with "weak" relationships (C and D).

nique at 6° per step (60 steps) for 40 min, with a 64 × 64 acquisition matrix and magnification factor of 1.5, using high-resolution parallel-hole collimators.

Image Reconstruction

The low-resolution cross-sectional images of ^{133}Xe and ECD were reconstructed using filtered backprojection and were corrected for attenuation. Furthermore, rCBF (ml/min/100 g) was calculated from ^{133}Xe SPECT data using the method of Kanno and Lassen (*19–21*). All images were displayed in a 64 × 64 matrix using a linear 16 shade color scale normalized to the highest flow value for ^{133}Xe or highest count density for ECD. Transverse resolution was 1.7 cm and axial resolution was 1.9 cm.

High-resolution images were reconstructed in the transverse plane using filtered backprojection with a fourth or fifth order Butterworth filter and a cutoff frequency of 0.3–0.4 cycles per pixel. Slices were attenuation corrected. Image sets were summed to a final slice thickness of 5–7 mm.

Data Analysis

Regional cerebral blood flow (^{133}Xe) and ECD count density were compared in 24 fixed ROIs applied to the low-resolution image 6 cm above the CML (Fig. 1) by the method of Stokely et al. (*22*). Regions were normalized to global cerebral blood flow (gCBF) for ^{133}Xe or global count density for ECD, derived from the hemispheric average in this slice. Profile plots were obtained of individual subjects and of average values for each region across subjects (mean ± s.d.). Linear regression analysis was used to examine the relationship between rCBF ratios and ECD count density ratios. Global flow or count density was also compared with cerebellar values since both are often employed in normalization schemes.

In addition, to explore whether or not the relationship between rCBF and ECD was dependent on absolute flow, ECD ROI data were expressed in units of ml/min/100 g, assuming equivalency between gCBF (^{133}Xe) and ECD global count density. That is, derived rCBF values for ECD ROI data were calculated from a scale factor equal to the ratio of gCBF (^{133}Xe) to the ECD global count density. Linear regression analysis then was used to examine the relationship between rCBF (ml/min/100 g) and derived ECD rCBF values (ml/min/100 g). As with count ratios, global and cerebellar values were also compared.

In five patients with well demarcated rCBF lesions, the lesion area also was outlined by visual inspection on the ^{133}Xe rCBF image and reproduced in the ECD images by computer overlay. Linear regression analysis was used to examine the correlation of lesion detection by derived ECD rCBF to that of ^{133}Xe rCBF.

Finally, in a subset of six subjects, high-resolution images were repeated up to 4 hr postinjection. The rate of clearance of ECD from gray and white matter was calculated relative to the first high-resolution image obtained in each subject (≈45 min postinjection).

RESULTS

The radiopharmaceutical purity of ^{99m}Tc-ECD established by thin-layer chromatography was >95% in all samples (18 kits).

Blood and urine chemistries were unchanged from pre-ECD values in all subjects up to seven days postinjection. Similarly, vital signs were unaffected by the administration of ECD. Subjects did not report any adverse reactions to ECD, nor were any noted by the investigators.

Profile plots comparing rCBF (^{133}Xe) ratios and ECD count density ratios for two subjects with "close" relationships are shown in Figures 2A and 2B, and for two subjects with "weak" relationships in Figures 2C and 2D. There is substantial agreement in the pattern of relative distribution between rCBF and ECD uptake within subjects. The relative distribution of the two radiopharmaceuticals averaged across subjects is shown in Figure 3.

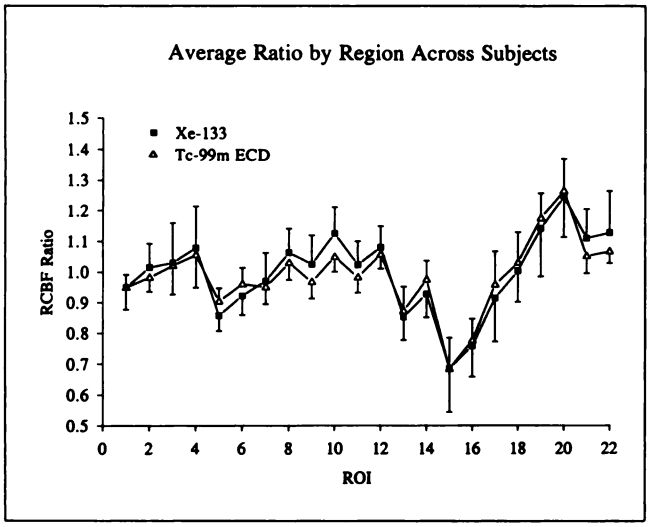

FIGURE 3. Relative distribution of ^{133}Xe and ^{99m}Tc-ECD averaged across subjects.

There were no consistent areas of disagreement across subjects. No statistically significant differences were noted in any region. Xenon-133 and ECD ratios for each subject in each region were subtracted to produce difference scores. When averaged across subjects by region, no difference score significantly deviated from zero ($p = 0.43$, paired t-test).

The results of linear regression analysis comparing rCBF ratios to ECD count density ratios are shown in Figure 4A. A significant correlation was observed ($r = 0.77$) with a slope of 0.64 ± 0.03 and an intercept of 0.36 ± 0.03. Since ECD and HMPAO have been reported to underestimate high rCBF, we performed separate regressions (Fig. 4B) on "low" ratio data (<1 for ^{133}Xe) and "high" ratio data (≥1 for ^{133}Xe). Neither the slope (0.62) nor the intercept (0.37) of the regression on "high" ratios were different from those for the whole data set. However, for the "low" ratios the slope increased to 0.73 and the intercept fell to 0.28. Partly due to the reduction in sample size, split regressions were substantially weaker.

The results of regression analysis comparing rCBF (ml/min/100 g, ^{133}Xe) with derived ECD rCBF (ml/min/100 g) are shown in Figure 5A. A closer correlation ($r = 0.88$) was found for these data than for the count ratio data. Also, this slope was closer to 1 ($m = 0.83 \pm 0.03$) than that for the ratio data and the intercept was closer to 0 ($b = 8.2 \pm 1.3$). These data were also subjected to separate low rCBF and high rCBF regression analyses (Fig. 5B), splitting the data at the mean ^{133}Xe rCBF value (51 ml/min/100 g). In this case, the slopes and intercepts of the high and low flow sets are not different from those of the complete data set. Thus, the derived ECD rCBF data suggest a mild underestimate of high flow by ECD, but not one as substantial as the count density ratio data might imply.

Global and cerebellar flow values (^{133}Xe) are compared in Figure 6A. They are essentially collinear ($m = 0.99$, $b = 4.6$), though there is some scatter in the data ($r = 0.84$). By contrast, when global and cerebellar ECD count densities are compared (Fig. 6B), the slope is <1 (0.78) despite a strong correlation ($r = 0.91$). This result suggests that cerebellar count density underestimates global count density at higher values. Since global count density can be increased as a result of either higher global flow or higher injected dose, we compared derived ECD rCBF for cerebellum to ^{133}Xe gCBF (Fig. 6C). This comparison removes the effects of variability in injected dose. The slope (1.04), intercept (6.2) and correlation coeffi-

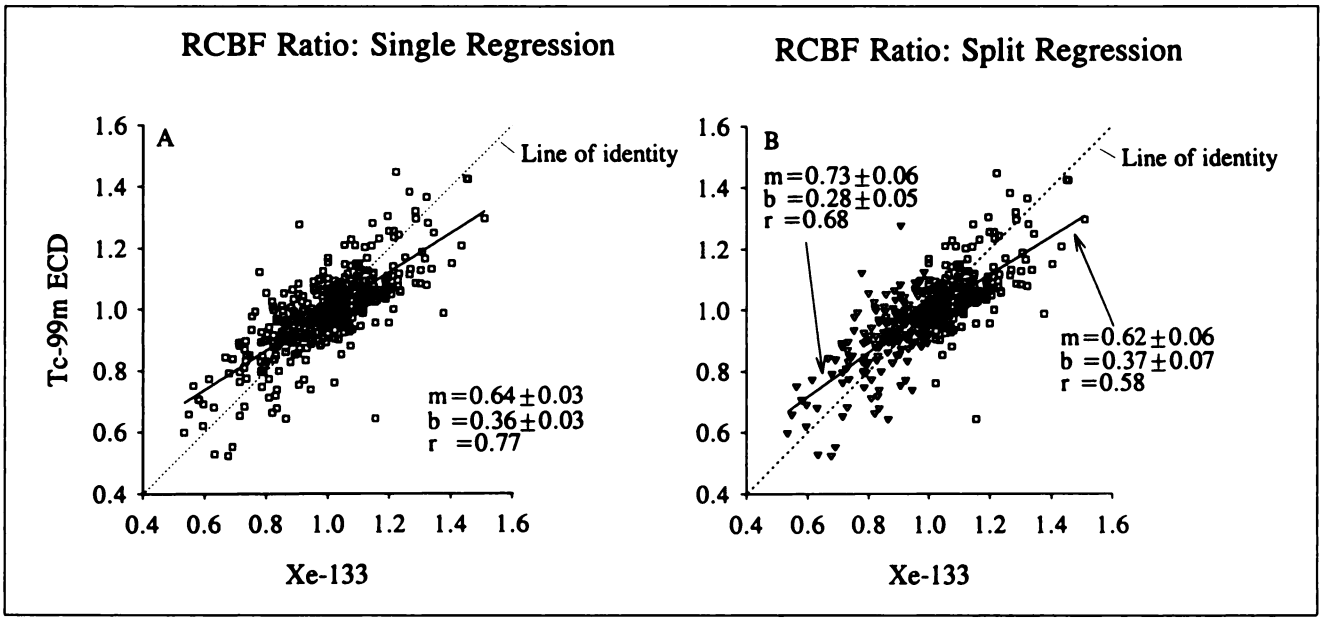

FIGURE 4. (A) Linear regression analysis comparing rCBF ratios to ECD count density ratios. (B) Split regression analyses on "low" ratio data (<1 for ^{133}Xe) and "high" ratio data (≥1 for ^{133}Xe).

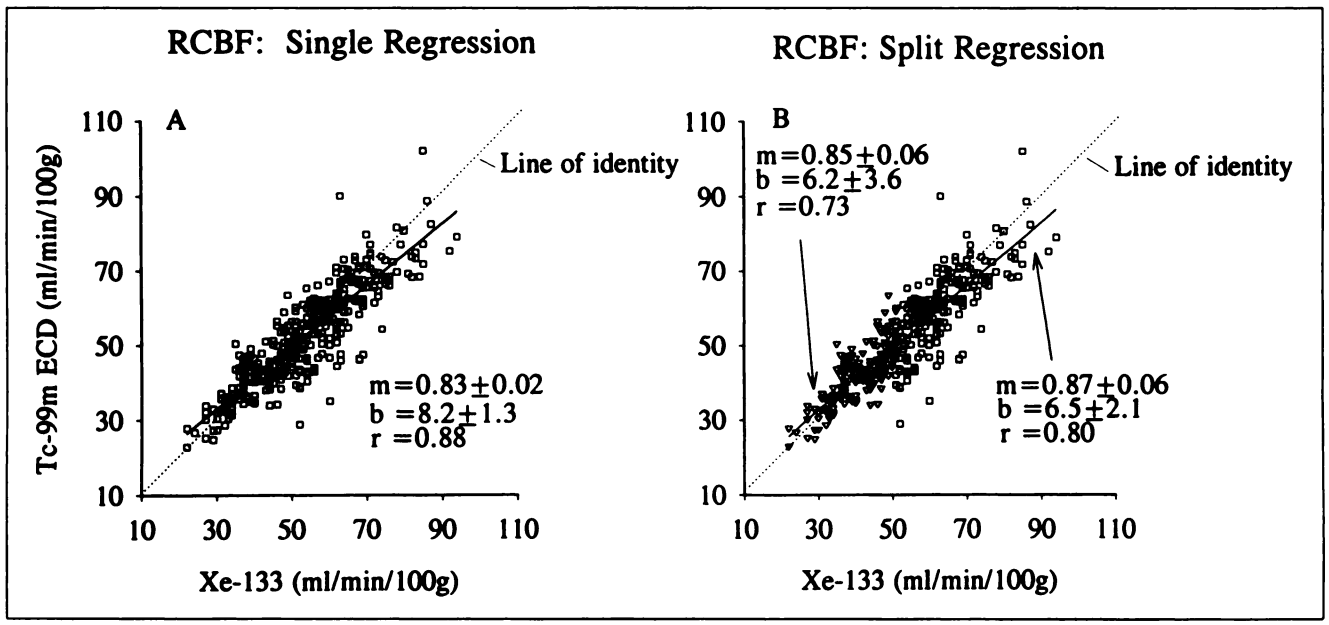

FIGURE 5. (A) Regression analysis comparing rCBF (ml/min/100 g, ^{133}Xe) to derived ECD rCBF (ml/min/100 g). (B) Split regression analyses on "low" rCBF (<51 for ^{133}Xe) and "high" rCBF (≥51 for ^{133}Xe).

cient (0.82) are identical to those obtained for ^{133}Xe cerebellar rCBF.

The data from five subjects with well demarcated perfusion deficits were used to calculate lesion rCBF for both ECD and ^{133}Xe. A significant correlation was observed between ECD-derived rCBF and ^{133}Xe rCBF in the lesion area (r = 0.92, Fig. 7). The slope (0.80) suggested a slight underestimation of lesion flow by ECD.

ECD clearance data for cortical gray matter ROIs derived from high-resolution scans are shown in Figure 8. Cortical clearance is slow (2.4%/hr) 1–4 hr postinjection. Similar values were found for subcortical gray matter and white matter ROIs.

DISCUSSION

Technetium-99m-ECD was reconstituted with consistent high purity. It also appears to be a safe radiopharmaceutical, producing no alterations in either blood or urine chemistries. Also, no adverse effects were reported by any subject. Similar findings were reported by Walovitch et al. (*16*) and Leveille et al. (*17*).

Individual profile plots comparing ECD and ^{133}Xe ratios revealed that the individual distribution pattern was the same for both tracers in all subjects (Fig. 2A–D). When subjects were grouped (Fig. 3), the overall pattern of distribution was again the same between the two phar-

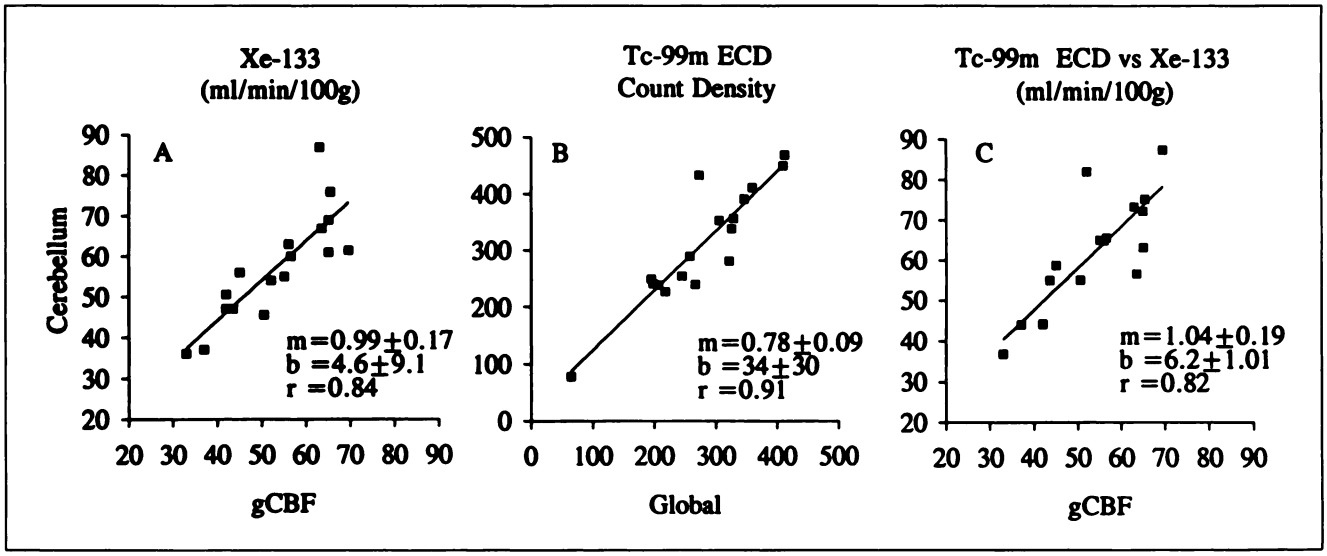

FIGURE 6. (A) Regression analysis comparing global and cerebellar flow (^{133}Xe). (B) Similar data comparing global and cerebellar ^{99m}Tc ECD count density. (C) Comparison of derived ECD cerebellar rCBF to ^{133}Xe gCBF.

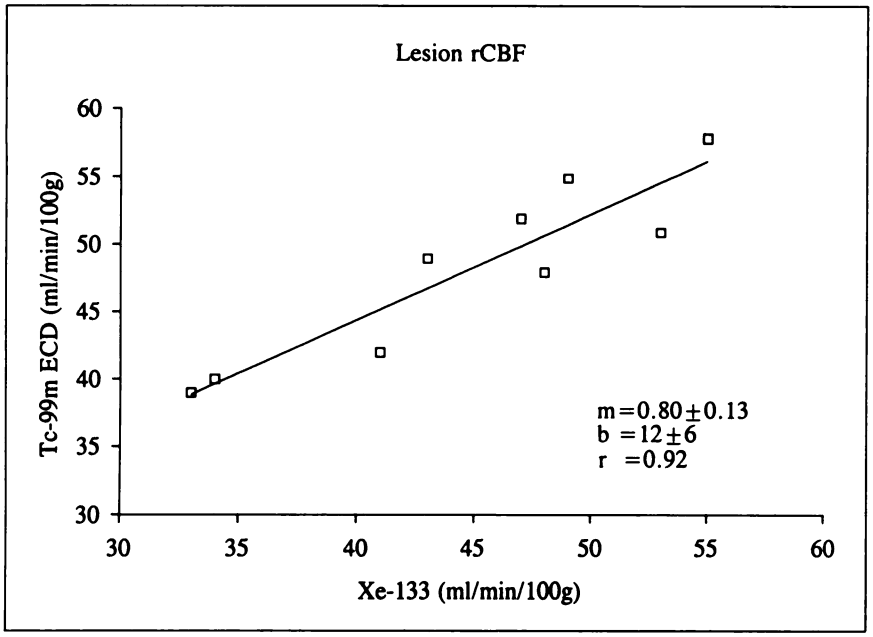

FIGURE 7. Regression analysis comparing derived ECD lesion rCBF to ^{133}Xe lesion rCBF.

maceuticals. Although variability did exist across subjects by region, no statistically significant differences in regional values were found between ^{99m}Tc-ECD and ^{133}Xe.

A linear relationship was observed in the regional distribution of ECD count density and ^{133}Xe rCBF ratio data (Fig. 4A). The slope (0.64) was <1, indicating that ECD may underestimate high flow; the positive intercept (0.36) may indicate that ECD overestimates low flow. Separate regression analyses of "high" and "low" ratio data (Fig. 4B) support this concept. Similar results (slope = 0.64) were reported by Costa et al. (*23*) in a comparison in dogs of ^{99m}Tc-HMPAO uptake to rCBF derived from tracer microspheres.

However, it is important to note that ratio data do not in fact reflect "high" or "low" flow values, but only relative values within a subject centered around that subject's global flow. In our subjects, gCBF varied from 35 to 70 ml/min/100 g. Consequently, a region with a high flow ratio in a subject with low gCBF might have an absolute value lower than that of a region with a low flow ratio in a subject with high gCBF.

Because there was an absolute measure of gCBF in each subject (^{133}Xe SPECT), it was possible to "calibrate" global ECD count density in units of ml/min/100 g. Although this approach may be less satisfactory than kinetic modeling of ECD uptake and retention by arterial blood sampling and rapid dynamic tomography, it is a reasonable and practical approximation to obtain absolute flow values for ECD. Furthermore, this approach removes effects of inter-individual variability in the relationship between injected dose and the percent of cardiac output going to the brain.

The regression of ECD-derived rCBF against ^{133}Xe rCBF, using this approach, yielded a slope closer to one (Fig. 5A). However, both single and split high/low flow regressions support the concept that ECD mildly underestimates rCBF at the upper end of the normal resting range. In contrast, Kuhl et al. (*24*) demonstrated a slope of one when comparing rCBF derived from tracer microspheres to rCBF derived from ^{125}I-IMP using a microsphere model in dogs. However, in the report of Kuhl et al., rCBF did not exceed 60 ml/min/100 g.

Since r values close to one ("good" correlations) could conceal true discrepancies regarding the relationship between these two rCBF tracers, two points should be considered regarding the data in Figure 5. First, we believe there are no subsets of the data with systematic variations (induced by the experiment) from the linear relationship seen in the total data set. That is, no brain

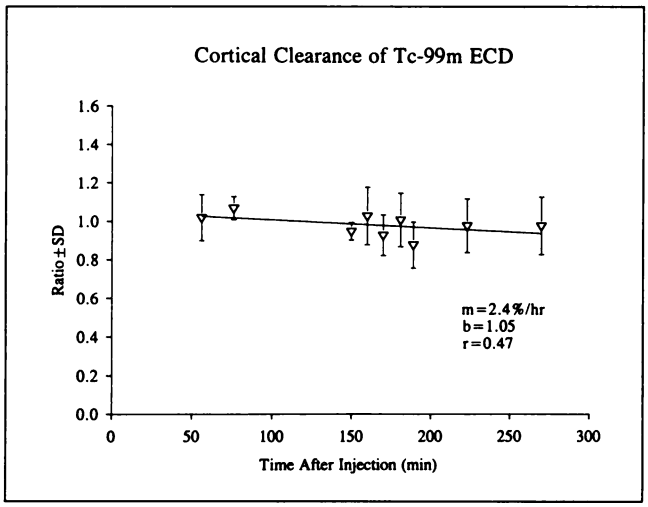

FIGURE 8. ECD clearance from cortical gray matter ROIs (derived from high-resolution scans). Ratios are relative to initial scans obtained 45 min after injection.

region consistently differed from other regions in its response to the two tracers (Fig. 3); there were no significant outliers and there were no positional effects since subjects did not move between ^{133}Xe and ECD acquisitions. Second, these data intentionally address only a limited range of flows from moderately reduced to the upper end of normal resting values. The inclusion of data from very low flow states (e.g., stroke) or from very high flow states (e.g., vasodilation with acetazolamide or during a seizure) might demonstrate nonlinearities. Thus, these data should not be overinterpreted.

Many investigators normalize regional values to the cerebellum instead of the whole brain. We explored the relationship between global and cerebellar data for ^{133}Xe and ECD (count density or derived rCBF) (Fig. 6A–C). The relationship of ^{133}Xe gCBF to cerebellar rCBF was linear (r = 0.84) with a slope (0.99) and intercept (4.6) not different from the line of identity. Thus, for ^{133}Xe, normalization to the cerebellum should be equivalent to normalization to gCBF. For ECD count density data, the relationship was also linear (r = 0.91) with a slope <1 (0.78) (Fig. 6B), indicating that normalization to the cerebellum for ECD would yield higher overall count ratios than normalization to the whole brain. These data also suggest that the cerebellum (predominantly gray matter) does not increase in ECD uptake at the same rate as whole brain (a mixture of gray and white matter).

However, count density is affected by both absolute flow and total injected dose. The comparison of derived cerebellar rCBF to true gCBF (^{133}Xe), which removes the effects of injected dose, yielded a slope (1.04) and intercept (6.2) not significantly different from the line of identity. The correlation coefficient (0.82) was equivalent to that for ^{133}Xe (0.84).

To further pursue the comparison of whole brain and cerebellum as reference tissues, we computed derived ECD rCBF values by calibrating cerebellar count density to ^{133}Xe cerebellar rCBF (Fig. 9). There was a linear relationship similar to that shown in Figure 5A where the whole brain was used as the reference tissue. Slope and intercept (m = 0.85, b = 6) were not different from whole brain data, but there was substantially greater scatter (r = 0.88 for whole brain, r = 0.75 for cerebellum). One factor that might contribute to increased scatter is the variability in cerebellar sampling caused by the limited resolution, incomplete sampling (only three slices) and the minimal positioning capability of the Tomomatic 64.

ECD uptake in mild to moderate perfusion defects was linearly related (r = 0.92) to ^{133}Xe rCBF in the same lesions (Fig. 7), with m = 0.80 and b = 12. As one might expect from Figures 4–6, low flow states (lesions) are detected by ECD, although their flow may be somewhat overestimated (reduced lesion contrast relative to ^{133}Xe). Similar findings have been reported for HMPAO relative to IMP (*7*) and for IMP relative to PET measures of rCBF (*25*). Although Nakano et al. (*7*) reported that IMP had superior lesion contrast to HMPAO, when lesion-to-normal tissue ratios for both agents were compared to that for ^{133}Xe, a linear correlation with a slope of one and intercept of zero was obtained.

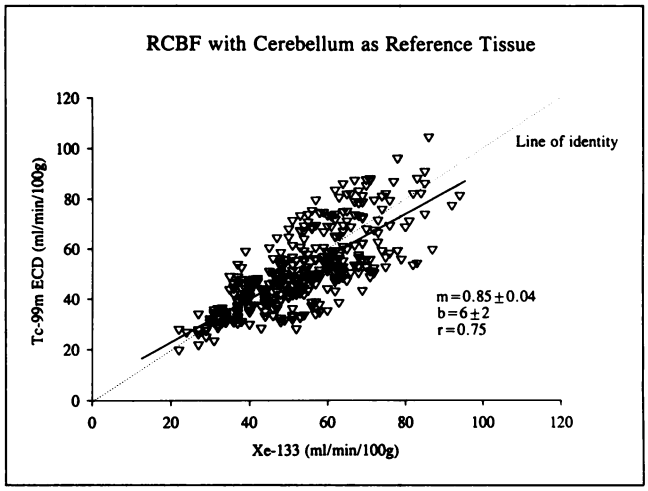

FIGURE 9. Comparison of derived ECD rCBF to ^{133}Xe rCBF using the cerebellum as the reference tissue.

Nishizawa et al. (*25*) compared IMP lesion flow to rCBF lesion flow and reported a slope closer to one (0.88) than the slope we measured for ECD. This is consistent with better estimation of lesion contrast for IMP than for ECD or HMPAO. Thus, while it appears that lesion detection follows the order (best to worst), i.e., ^{133}Xe > IMP > HMPAO = ECD, the quantitative differences may be small.

This interpretation should be made with an understanding of the limitations imposed by comparing diffusible (^{133}Xe) with nondiffusible (ECD) tracers. For example, rCBF computed from ^{133}Xe clearance data depends only on the rate of change of counts over time (slope). Thus, these images are not as sensitive to partial volume effects as are count-based images. Unfortunately, they do have significant problems with the estimate of white matter flow (regions not included in the data analyzed for this report). In contrast, count-based images such as those obtained from ECD have significant partial volume effects in cortex if image resolution is poor, but can faithfully monitor flow to large white matter zones. We attempted to minimize this problem by using the same tomograph and collimators for both tracers, but interpretative caution is warranted.

Another caution should be considered. At a recent symposium (Copenhagen, July 1992), several groups (Nakagawara et al. and Lassen et al., *personal communications*) reported that ECD did not follow hyperemia or luxury perfusion in selected stroke cases. This phenomenon is not yet understood, but it clearly illustrates that some pathologic conditions would not demonstrate the correlation between ECD uptake and ^{133}Xe rCBF found in our subjects. For the circumstances of sub-acute stroke, this may turn out to be an advantage of ECD. In

other circumstances, the coupling (or decoupling) of ECD uptake to rCBF must be demonstrated.

High-resolution SPECT measurement of ECD clearance over time demonstrated that there is only a 2.4%/hr cortical loss of ECD during the first few hours. Similar results were obtained for subcortical gray and white matter ROIs. A sharper decline (5%–7% from 20 min to 70 min) was reported by Leveille et al. (*17*). The most likely explanation for the difference between our data and that of Leveille et al. is that our data are measured relative to a first scan obtained 45 min postinjection, while their data are measured relative to a first scan only 20 min postinjection. Thus, there may be a phase of early rapid clearance in the first 45 min followed by a prolonged stable period of slow clearance (equally from all compartments). These findings would argue for beginning ECD scans no sooner than 45 min postinjection.

In summary, ECD is a marker of regional cerebral perfusion. The distribution of ECD is linearly related to rCBF measured by ^{133}Xe SPECT, although our data suggest a mild underestimation of flow at the high end of the normal range. Normalization to global flow provides a less variable measure of relative rCBF than normalization to cerebellum, but the two reference tissues are colinear. Mild to moderate rCBF lesions are clearly detected by ECD, although (as has been reported for HMPAO) their contrast is not as high as with ^{133}Xe.

ACKNOWLEDGMENT

This research was supported in part by a grant from E.I. Du Pont de Nemours & Co.

REFERENCES

1. Kety SS, Schmidt CG. The nitrous oxide method for quantitative determination of cerebral blood flow in man: theory, procedure and normal values. *J Clin Invest* 1948;27:476–483.
2. Fick A. Ueber die Messung des Blutquantums in den Herzeventrikeln. *Verh Dtsch Phys Med Ges* 1870;2:16.
3. Winchell HS, Baldwin RM, Lin TH. Development of ^{123}I-labeled amines for brain studies: localization of ^{123}I-iodophenylalkylamines in rat brain. *J Nucl Med* 1980;21:940–202.
4. Neirinckx RD, Canning LR, Piper IM, et al. Technetium-99m-d,l-HMPAO: a new radiopharmaceutical for SPECT imaging of regional cerebral blood perfusion. *J Nucl Med* 1987;28:191–202.
5. Nowotnik DP, Canning LR, Cumming SA, et al. Development of a ^{99m}Tc-labeled radiopharmaceutical for cerebral blood flow imaging. *Nucl Med Commun* 1985;6:499–506.
6. Devous MD Sr, Stokely EM, Bonte FJ. Quantitative imaging of regional cerebral blood flow in man by dynamic single-photon tomography. In: BL Holman, ed, *Radionuclide imaging of the brain*. New York: Churchill Livingstone; 1985:135–162.
7. Nakano S, Kinoshita K, Jinnouchi S, Hiroaki H, Watanabe K. Comparative study of regional cerebral blood flow images by SPECT using xenon-133, iodine-123-IMP, and technetium-99m-HMPAO. *J Nucl Med* 1989;30:157–164.
8. Ell PJ, Jarritt PH, Costa DC, Cullum ID, Lui D. Functional imaging of the brain. *Semin Nucl Med* 1987;17:214–229.
9. Lassen NA, Henriksen L, Holm S, et al. Cerebral blood-flow tomography: xenon-133 compared with isopropyl-amphetamine-iodine-123: concise communication. *J Nucl Med* 1983;24:17–21.
10. Leonard J-P, Nowotnik DP, Neirinckx RD. Technetium-99m-d,l-HMPAO: a new radiopharmaceutical for imaging regional brain perfusion using SPECT—a comparison with iodine-123-HIPDM. *J Nucl Med* 1986;27:1819–1823.
11. Lassen NA, Andersen AR, Friberg L, Paulson OB. The retention of ^{99m}Tc-d,l-HMPAO SPECT in the human brain after intracarotid bolus injection: a kinetic analysis. *J Cereb Blood Flow Metab* 1988;8:S13–S22.
12. Holm S, Andersen AR, Vorstrup S, Lassen NA, Paulson OB, Holmes RA. Dynamic SPECT of the brain using a lipophilic technetium-99m complex, PnAO. *J Nucl Med* 1985;26:1129–1134.
13. Bok BD, Scheffel U, Goldfarb HW, et al. Comparison of ^{99m}Tc complexes (NEP-DADT, ME-NEP-DADT and HMPAO) with ^{123}IAMP for brain SPECT imaging in dogs. *Nucl Med Commun* 1987;8:631–641.
14. Ballinger JR, Gulenchyn KY, Reid RH. Radiopharmaceutical factors in the variable quality of ^{99m}Tc-HMPAO images of the brain. *J Nucl Med* 1990;31:118–122.
15. Kung HF, Guo YH, Yu C-C, Billings J, Subramanyam V, Calabrese J. New brain perfusion imaging agents based on ^{99m}Tc-bis(aminoethanethiol) complexes: stereoisomers and biodistribution. *J Med Chem* 1989;32:437–444.
16. Walovitch RC, Hill TC, Garrity ST, et al. Characterization of ^{99m}Tc-1,1-ECD for brain perfusion imaging, part 1: pharmacology of technetium-99m ECD in nonhuman primates. *J Nucl Med* 1989;30:1892–1901.
17. Leveille J, Demonceau G, De Roo M, et al. Characterization of ^{99m}Tc-1,1-ECD for brain perfusion imaging, part 2: biodistribution and brain imaging in humans. *J Nucl Med* 1989;30:1902–1910.
18. Bonte FJ, Stokely EM. Single-photon tomographic study of regional cerebral blood flow after stroke: concise communication. *J Nucl Med* 1981;22:1049–1053.
19. Kanno I, Lassen NA. Two methods for calculating regional cerebral blood flow from emission computed tomography of inert gas concentrations. *J Comput Assist Tomogr* 1979;3:71–76.
20. Celsis P, Goldman T, Henriksen L, Lassen NA. A method for calculating regional cerebral blood flow from emission computerized tomography of inert gas concentrations. *J Comput Assist Tomogr* 1981;5:641–645.
21. Smith GT, Stokely EM, Lewis MH, Devous MD, Bonte FJ. An error analysis of the double-integral method for calculating brain blood perfusion from inert gas clearance data. *J Cereb Blood Flow Metab* 1984;4:61–67.
22. Stokely EM, Totah J, Homan R, Devous MD, Bonte FJ. Interactive graphics methods for regional quantification of tomographic brain blood flow images. *Proc Medcomp* 1982;IEEE:316–318.
23. Costa DC, Jones BE, Steiner TJ, et al. Relative ^{99m}Tc-HMPAO and ^{113}Sn-microspheres distribution in dog brain. *Nuklearmedizin* 1986;25:A53.
24. Kuhl DE, Barrio JR, Huang SC, et al. Quantifying local cerebral blood flow by N-isopropyl-p-[^{123}I] iodoamphetamine (IMP) tomography. *J Nucl Med* 1982;23:196–203.
25. Nishizawa S, Tanada S, Yonekura Y, et al. Regional dynamics of N-isopropyl-(^{123}I)p-iodo-amphetamine in human brain. *J Nucl Med* 1989;30:150–156.